Supplementary information

Theoretical design principles of metal catalysts for selective ammonia oxidation from high throughput computation

Jiaqiang Yang,[a] Xi Chen,[a] Zhang Liu,[a] Qingbo Wang,[b] Yanwei Wen,[a] Aimin Zhang,[c] Rong Chen*[,d] and Bin Shan*[,a]

[a] *State Key Laboratory of Material Processing and Die and Mould Technology and School of Materials Science and Engineering, Huazhong University of Science and Technology, Wuhan 430074, Hubei, China*

[b] *School of Mathematics and Physics, China University of Geosciences (Wuhan), Wuhan 430074, PR China*

[c] *State Key Laboratory of Advanced Technologies for Comprehensive Utilization of Platinum Metals, Kunming Institute of Precious Metals, Kunming 650106, China*

[d] *State Key Laboratory of Digital Manufacturing Equipment and Technology and School of Mechanical Science and Engineering, Huazhong University of Science and Technology, Wuhan 430074, Hubei, China*

The benchmark about cutoff energy in DFT calculation.

Table S1. The energy of bulk metal systems with different cutoff energy (*Ecut*) for DFT calculation (Unit: eV).

Ecut	Ag-fcc	Au-fcc	Cu-fcc	Ir-fcc	Pd-fcc	Pt-fcc	Rh-fcc	Ru-hcp
300eV	-10.830	-12.781	-14.781	-35.429	-20.912	-24.330	-29.163	-18.604
400eV	-10.796	-12.759	-14.779	-35.427	-20.891	-24.314	-29.147	-18.599
500eV	-10.795	-12.758	-14.772	-35.428	-20.892	-24.315	-29.148	-18.599

The adsorption behaviors on low index facet of different metal systems.

Table S2. The adsorption energies of reactants, intermediates and productions in NH_3-SCO process on low-index facets of Ag, Au, Ir, Cu, Pd, Pt, Rh and Ru (Unit: eV)

	NH_3^*	NH_2^*	NH^*	N^*	H^*	O^*	OH^*	O_2^*	H_2O^*	N_2^*	NO^*	N_2O^*
Ag(100)	-0.38	-1.98	-2.82	-2.92	-1.98	-0.87	-2.93	-0.63	-0.10	-0.01	-0.51	-0.03
Au(100)	-0.50	-2.11	-2.46	-2.55	-2.33	-0.02	-2.21	-0.14	-0.07	-0.01	-0.64	-0.03
Ir(100)	-1.27	-3.56	-4.71	-5.48	-2.97	-2.15	-3.54	-	-0.32	-0.76	-2.63	-0.78
Cu(100)	-0.60	-2.63	-4.11	-4.70	-2.43	-2.00	-3.35	-1.05	-0.17	-0.09	-1.21	0.01
Pd(100)	-0.79	-2.71	-4.09	-5.07	-2.77	-1.20	-2.76	-1.04	-0.17	-0.37	-2.20	-0.22
Pt(100)	-1.09	-3.20	-3.83	-4.61	-2.91	-1.31	-3.07	-1.21	-0.14	-0.47	-2.30	-0.25
Rh(100)	-1.02	-3.30	-5.04	-5.89	-2.85	-2.28	-3.37	-2.00	-0.28	-0.72	-2.78	-1.06
Ag(111)	-0.30	-1.64	-2.24	-1.96	-2.06	-0.25	-2.59	0.18	-0.07	0.00	-0.25	-0.02
Au(111)	-0.33	-1.48	-2.28	-2.37	-2.18	0.19	-1.89	0.70	-0.05	0.01	-0.14	-0.01

Ir(111)	-0.95	-2.71	-4.44	-5.30	-2.71	-1.75	-2.73	-1.07	-0.13	-0.37	-2.00	0.04
Cu(111)	-0.48	-2.19	-3.42	-3.54	-2.48	-1.38	-3.03	-0.56	-0.09	0.01	-1.03	0.02
Pd(111)	-0.83	-2.54	-4.24	-5.05	-2.97	-1.55	-2.75	-0.96	-0.13	-0.29	-2.48	-0.06
Pt(111)	-0.89	-2.41	-4.02	-4.81	-2.73	-1.12	-2.35	-0.53	-0.08	-0.14	-1.76	0.44
Rh(111)	-0.97	-2.90	-4.64	-5.67	-2.85	-2.13	-3.14	-1.62	-0.39	-0.64	-2.59	-0.43
Ru(0001)	-0.95	-3.10	-5.20	-6.36	-2.91	-2.96	-3.60	-	-0.42	-0.66	-2.74	-0.89

Table S3. The binding types of reactants, intermediates and productions in NH_3-SCO process on low-index facets of Ag, Au, Ir, Cu, Pd, Pt, Rh and Ru.

	NH_3^*	NH_2^*	NH^*	N^*	H^*	O^*	OH^*	O_2^*	H_2O^*	N_2^*	NO^*	N_2O^*
Ag(100)	top	bridge	4-fold	4-fold	bridge	4-fold	4-fold	double	-	-	4-fold	-
Au(100)	top	bridge	4-fold	4-fold	bridge	4-fold	bridge	double	-	-	bridge	-
Ir(100)	top	bridge	4-fold	4-fold	bridge	4-fold	bridge	-	top	top	bridge	double
Cu(100)	top	bridge	4-fold	4-fold	4-fold	4-fold	4-fold	double	top	-	4-fold	-
Pd(100)	top	bridge	4-fold	4-fold	bridge	4-fold	4-fold	double	top	top	bridge	double
Pt(100)	top	bridge	4-fold	Bridge	bridge	4-fold	bridge	double	top	top	bridge	top
Rh(100)	top	bridge	4-fold	4-fold	bridge	4-fold	4-fold	double	top	top	bridge	double
Ag(111)	top	bridge	3-fold	3-fold	3-flod	3-fold	3-fold	double	-	-	3-fold	-
Au(111)	top	bridge	3-fold	3-fold	3-fold	3-fold	3-fold	double	-	-	bridge	-
Ir(111)	top	bridge	3-fold	3-fold	3-fold	3-fold	bridge	double	-	top	3-fold	-
Cu(111)	top	bridge	3-fold	3-fold	3-fold	3-fold	3-fold	double	-	-	3-fold	-
Pd(111)	top	bridge	3-fold	3-fold	3-fold	3-fold	3-fold	double	-	top	3-fold	-
Pt(111)	top	bridge	3-fold	3-fold	3-fold	3-fold	bridge	double	-	top	3-fold	double
Rh(111)	top	bridge	3-fold	3-fold	3-fold	3-fold	3-fold	double	top	top	3-fold	double
Ru(0001)	top	bridge	3-fold	3-fold	3-fold	3-fold	3-fold	-	top	top	3-fold	double

Note: The "double" means double neighboring sites are needed for O_2 and N_2O adsorption because two atoms of molecules binds to surface atoms and "-" means the non-adsorption or non-chemisorption for O_2, H_2O, N_2 and N_2O molecules on metal catalysts.

Table S3 shows the stable binding for intermediates on metal catalysts. In general, NH_3^*, NH_2^*, NH^* and N^* and O^* prefer to bind to surface with top (top), bridge (bridge), 4-fold (3-fold), 4-fold (3-fold) and 4-fold (3-fold) types for (100) ((111)), respectively, due to the decreasing coordination atoms. Adsorbed H and OH mainly possess the bridge (bridge) and 4-fold (3-fold) binding for (100) ((111)). As for other reactants and products, H_2O and N_2 mainly possess the top binding and the double sites are needed for O_2 and N_2O adsorption. And the adsorbed NO is obtained through the N-metal interaction with bridge (bridge) and 4-fold (3-fold) binding for (100) ((111)).

The reaction information on different facets of metal systems.

Table S4. The detailed reaction barriers (E_a) and enthalpy (E_n) of elementary steps involved in NH_3-SCO at (100) (Units: eV).

	Ag(100)		Au(100)		Cu(100)		Ir(100)		Pd(100)		Pt(100)		Rh(100)	
	E_a	E_n	E_a	E_n	E_a	E_n	E_a	E_n	E_a	E_n	E_a	E_n	E_a	E_n

$NH_3^*+OH^*=NH_2^*+H_2O^*/H_2O(g)+^*$	0.68	0.65	1.15	0.24	0.82	0.57	1.18	0.00	0.91	0.22	1.09	0.04	1.32	0.32
$NH_2^*+OH^*=NH^*+H_2O^*/H_2O(g)+^*$	1.04	0.71	1.17	0.92	1.17	0.47	1.17	0.68	1.41	0.13	1.10	0.25	1.10	-0.09
$NH^*+OH^*=N^*+H_2O^*/H_2O(g)+^*$	1.21	0.91	1.03	0.38	2.30	0.87	1.47	0.56	1.61	-0.01	1.25	0.42	1.34	0.40
$NH_3^*+O^*=NH_2^*+OH^*$	0.77	-0.27	0.62	-0.52	0.92	-0.03	1.31	-0.13	0.79	-0.26	0.76	-0.25	1.02	-0.17
$NH_2^*+O^*=NH^*+OH^*$	1.00	0.06	0.74	0.15	1.30	0.07	0.97	0.47	1.09	-0.23	1.19	0.11	0.81	-0.09
$NH^*+O^*=N^*+OH^*$	2.55	-0.09	0.63	-0.19	2.17	0.43	0.81	0.16	1.57	-0.27	0.09	-0.13	1.46	0.34
$NH_3^*+^*=NH_2^*+H^*$	2.07	1.23	1.97	0.95	2.08	0.47	0.90	-0.37	1.50	0.19	1.69	-0.12	0.91	-0.25
$NH_2^*+^*=NH^*+H^*$	2.60	1.43	2.31	1.70	1.92	0.48	1.25	0.18	1.46	0.17	1.41	-0.76	1.09	-0.28
$NH^*+^*=N^*+H^*$	3.06	1.57	2.09	1.58	2.60	0.80	1.19	0.08	1.58	0.08	1.00	0.14	1.44	0.07
$N^*+O^*=NO^*+^*$	2.20	-0.86	0.75	-2.36	2.69	1.30	2.06	0.72	2.44	0.00	0.32	-0.63	2.57	1.24
$2N^*=N_2^*+*/N_2(g)+2^*$	1.82	-4.52	0.75	-5.63	2.39	-1.08	1.66	-0.19	4.25	-0.49	1.02	-1.60	3.54	0.86
$N^*+NO^*=N_2O^*+*/N_2O(g)+2*$	1.40	-2.57	0.97	-2.82	1.15	0.00	1.28	1.28	1.78	1.10	2.25	0.65	2.09	1.67
$O_2*+*=2O^*$	1.03	-1.22	0.57	-0.12	0.21	-2.96	-	-	0.38	-1.45	0.25	-1.41	0.27	-2.45
$NH_3+*=NH_3^*$	-	-0.38	-	-0.50	-	-0.60	-	-1.27	-	-0.79	-	-1.09	-	-1.02
$O_2+*=O_2^*$	-	-0.63	-	-0.14	-	-1.05		-4.28	-	-1.04	-	-1.21	-	-2.00
$NO^*=NO+*$	-	0.51	-	0.64	-	1.21	-	2.63	-	2.20	-	2.30	-	2.78
$N_2^*=N_2+*$	-	-	-	-	-	-	-	0.76	-	0.37	-	0.47	-	0.72
$N_2O^*=N_2O+*$	-	-	-	-	-	-	-	0.78	-	0.22	-	0.25	-	1.06
$H_2O^*=H_2O+*$	-	-	-	-	-	0.17	-	0.32	-	0.17	-	0.14	-	0.28
$O^*+H^*=OH^*+*$	0.91	-1.59	0.64	-1.36	1.23	-0.51	0.83	0.06	1.16	-0.30	0.56	-0.41	1.00	0.22
$2OH^*=H_2O^*+O^*/H_2O(g)+O^*+*$	0.61	0.54	0.59	0.36	0.55	0.26	0.77	0.13	0.58	0.29	1.26	0.10	0.54	0.19

Table S5. The detailed reaction barriers (E_a) and enthalpy (E_n) of elementary steps involved in NH_3-SCO at (111) (Units: eV).

	Ag(111)		Au(111)		Cu(111)		Ir(111)		Pd(111)		Pt(111)		Rh(111)		Ru(0001)	
	E_a	E_n	E_a	E_n	E_a	E_n	E_a	E_n	E_a	E_n	E_a	E_n	E_a	E_n	E_a	E_n
$NH_3^*+OH^*=NH_2^*+H_2O^*/H_2O(g)+^*$	1.05	0.57	0.91	0.12	0.68	0.38	1.15	0.24	0.73	0.03	1.08	0.15	0.92	0.23	1.54	0.67
$NH_2^*+OH^*=NH^*+H_2O^*/H_2O(g)+^*$	0.59	0.49	1.51	-0.11	0.56	0.43	0.76	-0.27	1.49	-0.19	0.60	-0.46	0.53	-0.05	2.13	0.06
$NH^*+OH^*=N^*+H_2O^*/H_2O(g)+^*$	1.03	0.74	0.75	-0.05	1.11	0.78	0.61	-0.06	0.31	-0.45	0.63	-0.37	0.88	-0.18	1.29	0.38
$NH_3^*+O^*=NH_2^*+OH^*$	0.70	0.04	0.99	0.23	0.79	0.11	1.37	0.37	1.29	0.49	1.28	0.41	1.37	0.51	1.19	0.36
$NH_2^*+O^*=NH^*+OH^*$	0.85	-0.03	1.42	-0.02	0.85	0.07	1.10	0.05	1.34	0.00	0.99	-0.10	1.13	0.06	0.86	-0.15
$NH^*+O^*=N^*+OH^*$	1.39	0.25	1.29	0.16	1.61	0.57	1.17	0.46	1.27	0.29	1.54	0.29	1.55	0.29	1.14	0.30
$NH_3^*+^*=NH_2^*+H^*$	2.19	1.47	2.46	1.61	1.83	0.67	1.64	0.44	1.50	0.24	1.49	0.66	1.59	0.10	1.25	-0.12
$NH_2^*+^*=NH^*+H^*$	2.35	1.61	3.23	1.40	1.56	0.58	1.19	-0.04	1.08	-0.28	1.32	0.03	1.42	-0.20	1.39	-0.17
$NH^*+^*=N^*+H^*$	2.69	2.02	2.23	1.70	2.13	1.27	1.26	0.37	1.47	0.12	1.76	0.41	1.22	0.03	0.85	-0.63
$N^*+O^*=NO^*+^*$	1.25	-2.12	1.25	-2.11	1.57	-0.36	2.00	0.49	2.36	-0.26	2.28	-0.19	2.58	0.87	3.23	2.06
$2N^*=N_2^*+*/N_2(g)+2^*$	0.96	-6.28	1.75	-5.51	0.99	-3.28	2.44	-0.39	2.40	-0.72	2.38	-1.01	1.67	0.19	3.06	1.42
$N^*+NO^*=N_2O^*+*/N_2O(g)+2*$	0.52	-3.73	0.07	-3.21	0.67	-1.33	2.04	1.30	2.03	1.37	1.53	0.90	2.15	1.77	2.14	2.07
$O_2*+*=2O^*$	0.95	-0.69	1.54	-0.36	0.19	-2.22	0.06	-2.30	0.63	-1.83	0.68	-1.54	0.10	-2.56	-	-
$NH_3+*=NH_3^*$	-	-0.30	-	-0.33	-	-0.48	-	-0.95	-	-0.83	-	-0.89	-	-0.97	-	-0.95
$O_2+*=O_2^*$	-	0.18	-	0.70	-	-0.56	-	-1.07	-	-0.96	-	-0.53	-	-1.62		-5.07
$NO^*=NO+*$	-	0.25	-	0.14	-	1.03	-	-2.00	-	-2.48	-	-1.76	-	2.59	-	2.74
$N_2^*=N_2+*$	-	-	-	-	-	-	-	0.37	-	0.29	-	-0.14	-	0.64	-	0.66
$N_2O^*=N_2O+*$	-	-	-	-	-	-	-	0.04	-	0.06	-	-	-	0.43	-	0.89

$H_2O^*=H_2O+*$	-	-	-	-	-	-	-	0.13	-	0.13	-	-	-	0.39	-	0.42
$O^*+H^*=OH^*+*$	0.66	-1.75	0.62	-1.39	0.87	-0.65	1.14	0.10	1.28	0.19	0.98	-0.08	1.24	0.21	1.50	0.61
$2OH^*=H_2O^*+O^*/H_2O(g)+O^*+*$	0.40	0.29	0.31	-0.33	0.59	0.11	0.39	-0.57	0.24	-0.45	0.63	-0.60	0.29	-0.41	0.36	-0.41

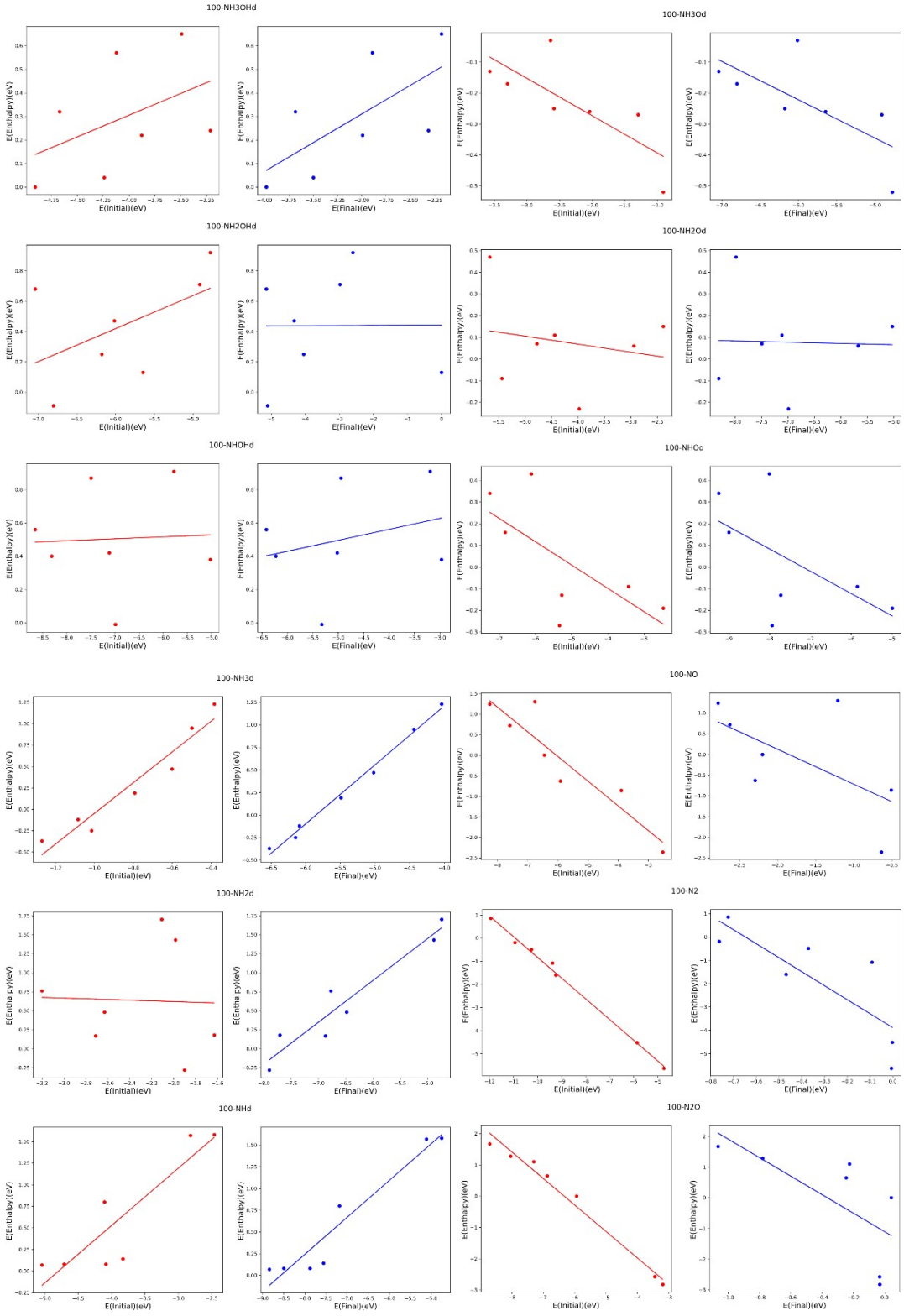

Fig. S1. The fitting relations between reaction enthalpy (E(enthalpy)) and binding energy (E(initial), E(final)) of reactants (initial states) and products (final states) for

direct, O-assisted and OH assisted NH_3 dissociation (denoted as NH_xd, NH_xOd and NH_xOHd, x=1, 2, 3) as well as NO, N_2 and N_2O formation (denoted NO, N_2 and N_2O) on (100).

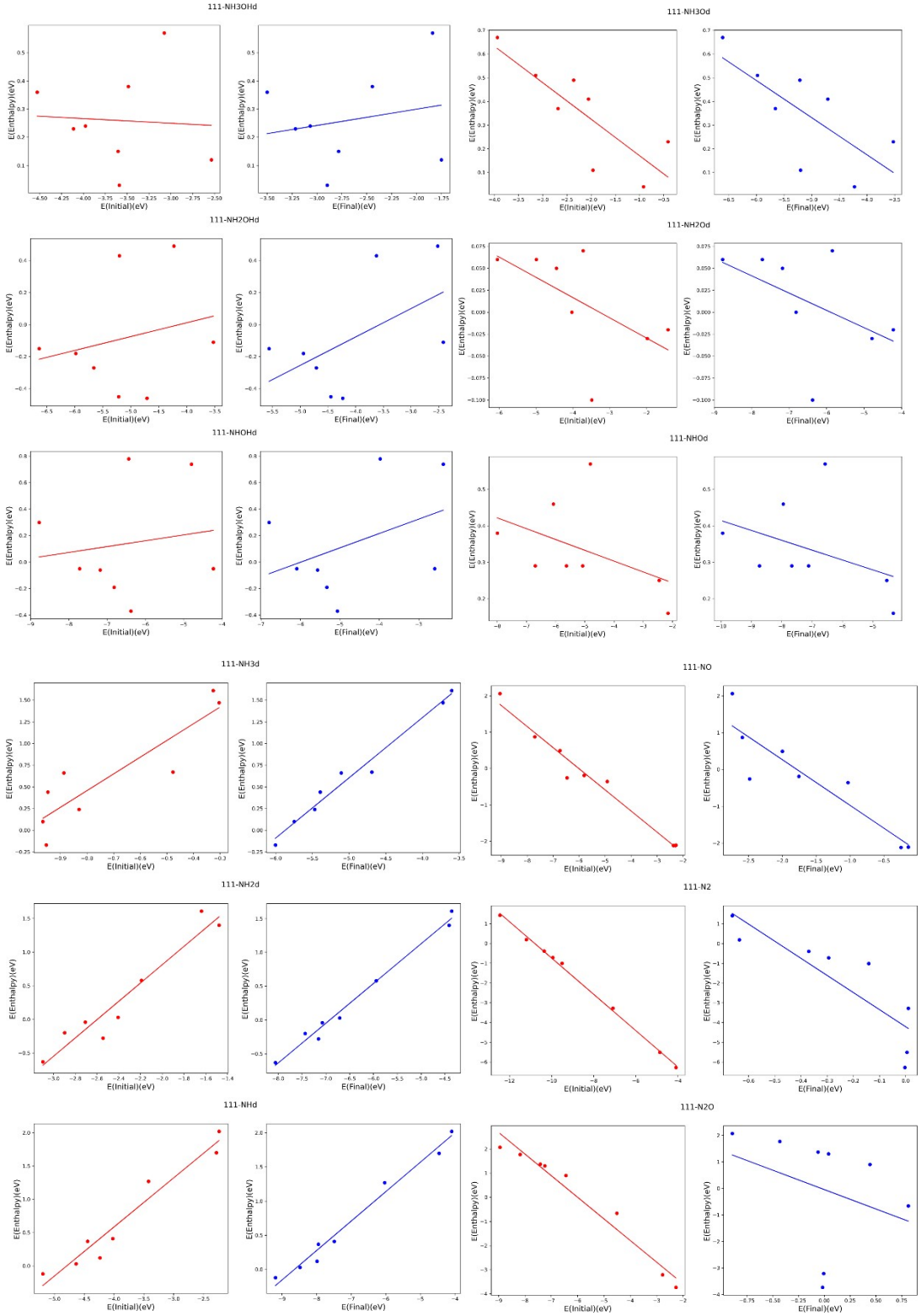

Fig. S2. The fitting relations between reaction enthalpy (E(enthalpy)) and binding energy (E(initial), E(final)) of reactants (initial states) and products (final states) for direct, O-assisted and OH assisted NH_3 dissociation (denoted as NH_xd, NH_xOd and

NH_xOHd, x=1, 2, 3) as well as NO, N_2 and N_2O formation (denoted NO, N_2 and N_2O) on (111).

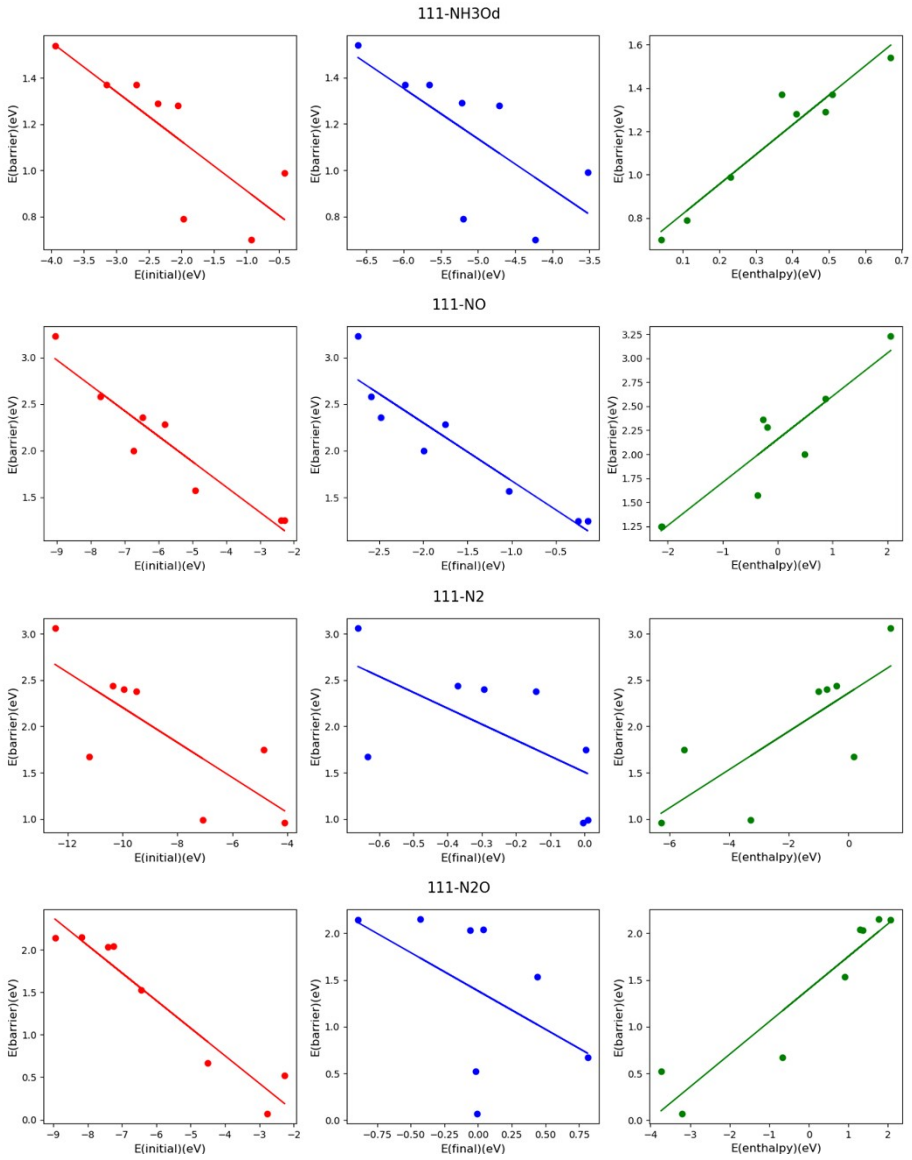

Fig. S3. The fitting relations of the barriers against the energy of initial and final states and enthalpy for O-assisted NH_3 scission and NO, N_2 and N_2O formation on (111), respectively.

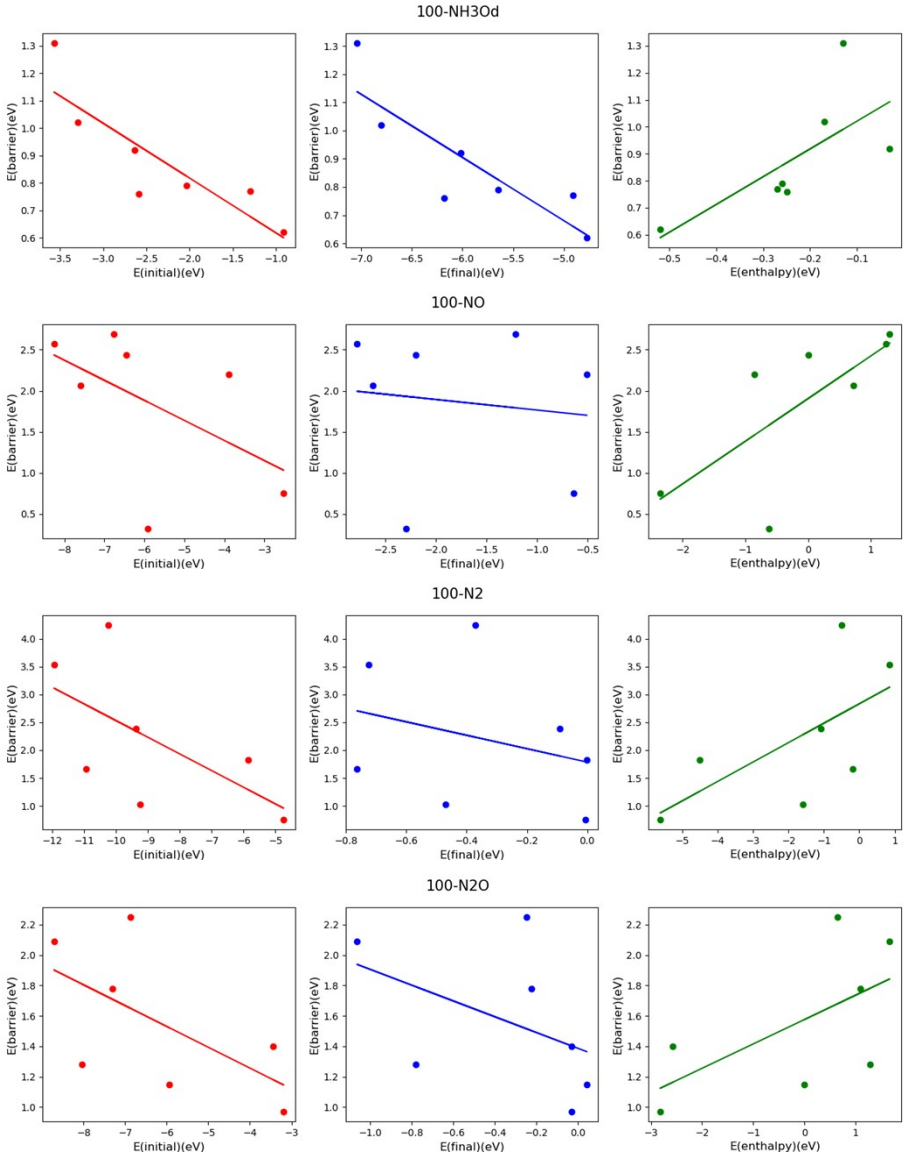

Fig. S4. The fitting relations of the barriers against the energy of initial and final states and enthalpy for O-assisted NH_3 scission and NO, N_2 and N_2O formation on (100), respectively.

The microkinetic results about metallic catalysts.

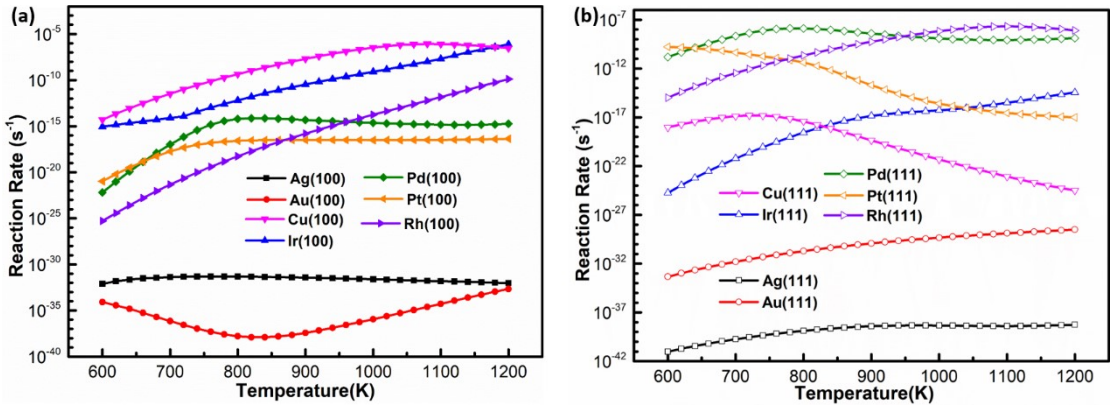

Fig. S5. The generation rates of N_2 on (100) and (111).

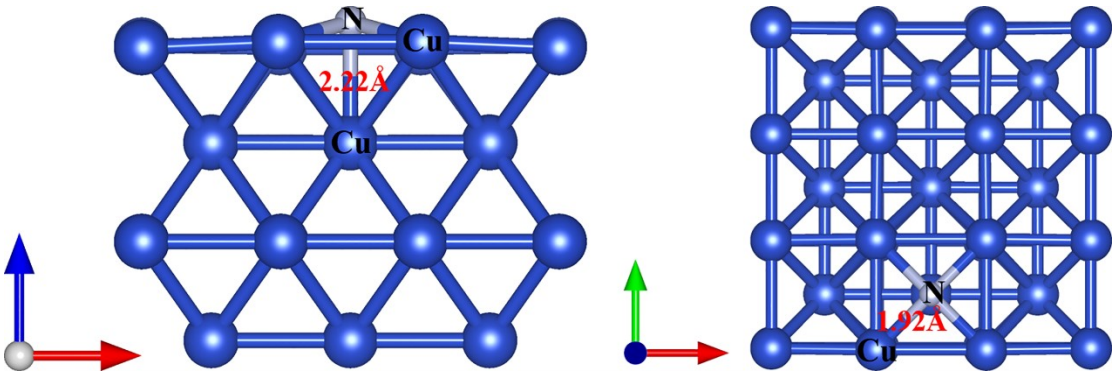

Fig. S6. The side and top views of binding configuration of N atom at Cu(100) facet.

The rate determining steps analysis on metallic catalysts.

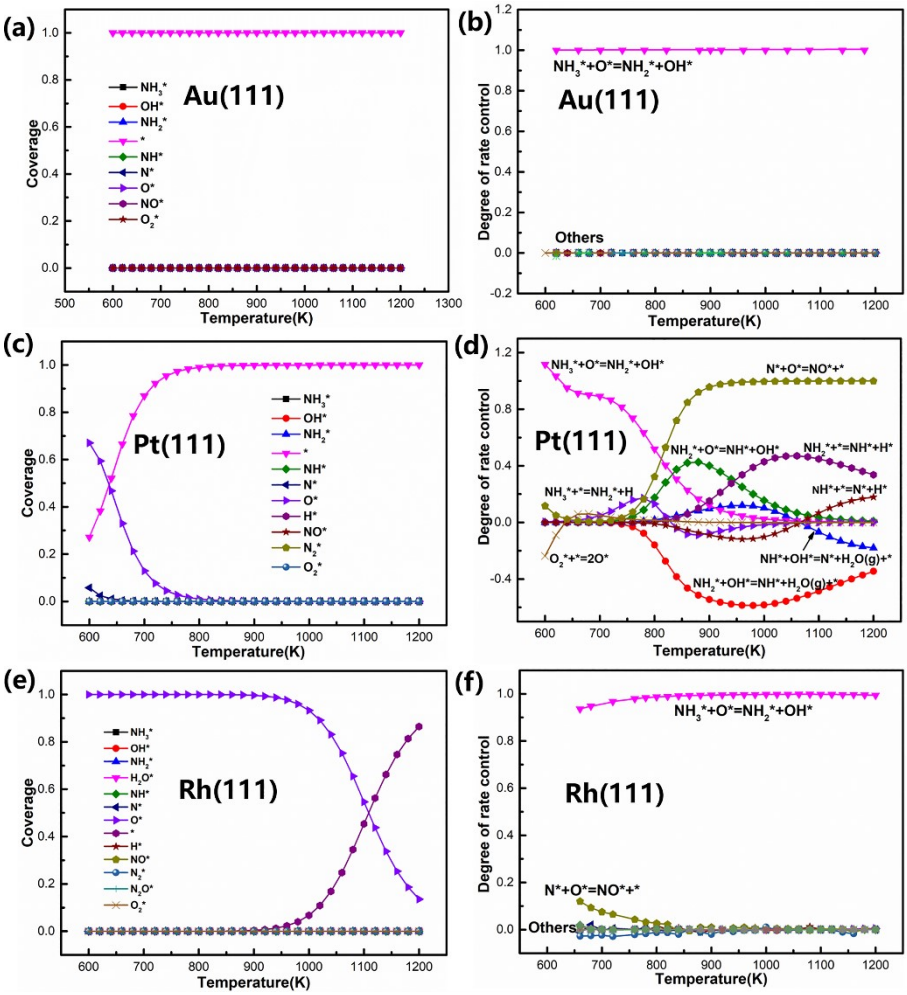

Fig. S7. The coverage and degrees of rate control of NH_3-SCO on representative Au(111), Pt(111) and Rh(111).

Au(111), Pt(111) and Rh(111) possess weak, moderate and strong N and O binding energy, respectively and thus could be reasonable representative of metal catalysts to figure out the rate-determining steps (RDS) of NH_3-SCO. Species coverage and degree of rate control (DRC) of elementary steps are calculated to identify the RDS,[1,2] as shown in Figure Sx. It is found in Fig. S7 (a) and (b) that for Au(111) with weak binding energy of intermediates, vacant site (*) is main intermediate and surface oxygen (O^*) assisted NH_3 dissociation ($NH_3^*+O^*=NH_2^*+OH^*$) becomes the RDS, which indicates that promoting the step through increasing the amounts of NH_3^* and O^* or decreasing the reaction barriers could achieve the enhancement of total reactivity. Then as for Pt(111) with moderate binding ability in Fig. S7 (c) and (d), the amount of O^* decreases until near to zero with increasing temperatures and vacant site (*) becomes the primary specie above 800 K. In the temperature zone (below 800K), $NH_3^*+O^*=NH_2^*+OH^*$ is primary RDS but the DRC gradually decreases with the temperature increasing, indicating the weaker and weaker influence on total reactivity. At the temperature above 800K, the formation of NO^* is the key RDS with positive enhancing effect on reactivity.

NH_2 scission also plays a key role that direct and O-assisted NH_2 scission possess the promoting effect while OH-assisted process exhibits the inhibition effect on NH_3-SCO. Finally, taking account of Rh(111) with the strong binding capacity for intermediates in Fig. S7 (e) and (f), it is seen that $NH_3^*+O^*=NH_2^*+OH^*$ is the primary RDS, which could be ascribed that plenty of surface O^* specie poisons the surface sites and inhibits the reaction proceeding. In general, it could be concluded that oxygen assisted NH_3 dissociation and the recombination of surface species for product formation are the key RDSs of NH_3-SCO for metal catalysts.

The origin of N_2 selectivity of Cu(100).

Table S6. The coverage of surface N and O species (***θ(N*) and θ(O*)***) at different temperatures for Cu(100) and Cu(111).

	Cu(100)		Cu(111)	
Temperature	***θ(N*)***	***θ(O*)***	***θ(N*)***	***θ(O*)***
500 K	5.01E-07	1.00	4.54E-12	1.00
600 K	1.08E-07	1.00	5.69E-12	1.00
700 K	5.85E-08	1.00	4.25E-12	0.90
800 K	3.62E-08	1.00	6.63E-13	0.27
900 K	2.38E-08	0.99	2.65E-14	0.03
1000 K	1.29E-08	0.87	1.24E-15	3.65E-03
1100 K	1.91E-09	0.39	8.43E-17	6.68E-04
1200 K	6.37E-11	0.08	9.21E-18	1.61E-04

The N_2 selectivity is defined as the ratio of N_2 formation rates and total NH_3 oxidation rates and the NH_3 oxidation rate should equal to the sum of N_2, NO and N_2O production rates. Taking account of N_2O formation from the recombination of surface N and NO species, N_2 and NO production processes become the keys influencing the selectivity. Therefore, we compare the reaction barriers and related N and O binding energy to reveal the factors of controlling the selectivity. Firstly, the difference between formation barriers of NO and N_2 ($\Delta E_{a,NO} - \Delta E_{a,N_2}$) are 0.30 and 0.58 eV for Cu(100) and Cu(111) respectively, which indicates N_2 formation is relative favorable in kinetics for Cu(100) and Cu(111), compared with NO formation. Then, it is found that Cu(100) exhibits stronger N and O atoms binding ability, which means that Cu(100) could provide more surface N and O species (Table S6). In the NH_3-SCO, more surface oxygen species could better assist the ammonia scission to produce more N species and enough surface N species could promote N_2 formation, Thus, it could be concluded that favorable N and O binding capacity are the keys of the superior N_2 selectivity of Cu(100). Finally, combining with the Figure of N_2 selectivity versus $E(N^*)$ and $E(N^*)+E(O^*)$ in manuscript (Fig. 9 of the manuscript), it is further found that oxygen binding ability is the feasible way for higher N_2 selectivity of Cu(111). Although Cu(100) possess comparable $E(N^*)$ compared with Pt(100), stronger oxygen binding prompts higher N_2 selectivity of Cu(100). Therefore, we believe that Cu(100) possesses relative strong oxygen binding ability and achieves the superior N_2 selectivity.

The information about binding energy of surface species on alloy catalysts.

Table S7. The binding energies of N and O atoms ($E(N^*)$ and $E(O^*)$, unit: eV) at (100) and (111) facets of different alloy systems.

	(100)			(111)		
	$E(N^*)$	$E(O^*)$	$E(N^*)+E(O^*)$	$E(N^*)$	$E(O^*)$	$E(N^*)+E(O^*)$
Ag_3Au_1	-2.891	-0.553	-3.444	-2.354	-0.340	-2.694
Ag_3Cu_1	-3.946	-1.709	-5.655	-2.936	-1.119	-4.055
Ag_3Pd_1	-4.033	-1.061	-5.094	-3.036	-0.692	-3.728
Ag_3Pt_1	-4.725	-1.196	-5.921	-3.670	-0.990	-4.660
Ag_3Ir_1	-7.279	-3.171	-10.450	-5.010	-1.786	-6.796
Ag_3Rh_1	-6.436	-2.453	-8.889	-4.658	-1.608	-6.266
Ag_3Ru_1	-8.398	-4.564	-12.962	-5.882	-2.602	-8.484
Au_3Ag_1	-2.827	-0.507	-3.334	-2.813	-0.331	-3.144
Au_3Cu_1	-3.718	-1.348	-5.066	-3.131	-0.844	-3.975
Au_3Pd_1	-3.934	-0.653	-4.587	-3.332	-0.421	-3.753
Au_3Pt_1	-4.650	-0.978	-5.628	-3.829	-0.721	-4.550
Au_3Ir_1	-6.190	-2.329	-8.519	-4.838	-1.390	-6.228
Au_3Rh_1	-5.789	-1.780	-7.569	-4.453	-1.099	-5.552
Au_3Ru_1	-6.868	-3.550	-10.418	-5.550	-2.263	-7.813
Cu_3Ag_1	-4.009	-1.672	-5.681	-3.637	-1.459	-5.096
Cu_3Au_1	-3.519	-0.961	-4.480	-3.396	-1.328	-4.724
Cu_3Pd_1	-4.499	-1.396	-5.895	-3.760	-1.644	-5.404
Cu_3Pt_1	-4.811	-1.236	-6.047	-3.976	-1.455	-5.431
Cu_3Ir_1	-6.676	-3.081	-9.757	-5.001	-1.861	-6.862
Cu_3Rh_1	-5.940	-2.277	-8.217	-4.782	-1.787	-6.569
Cu_3Ru_1	-7.073	-3.296	-10.369	-5.596	-2.439	-8.035
Pd_3Ag_1	-3.888	-0.853	-4.741	-4.817	-1.096	-5.913
Pd_3Au_1	-3.774	-0.407	-4.181	-4.752	-1.095	-5.847
Pd_3Cu_1	-4.673	-1.300	-5.973	-4.733	-1.269	-6.002
Pd_3Pt_1	-4.968	-1.166	-6.134	-5.046	-1.424	-6.470
Pd_3Ir_1	-6.081	-2.038	-8.119	-5.527	-1.849	-7.376
Pd_3Rh_1	-5.819	-1.950	-7.769	-5.490	-1.899	-7.389
Pd_3Ru_1	-6.954	-3.015	-9.969	-5.959	-2.375	-8.334
Pt_3Ag_1	-4.397	-1.068	-5.465	-5.076	-1.086	-6.162
Pt_3Au_1	-3.975	-0.600	-4.575	-4.882	-0.964	-5.846
Pt_3Cu_1	-4.420	-1.203	-5.623	-4.980	-1.309	-6.289
Pt_3Pd_1	-4.689	-1.150	-5.839	-5.069	-1.297	-6.366
Pt_3Ir_1	-5.198	-1.819	-7.017	-5.230	-1.532	-6.762

Pt_3Rh_1	-5.079	-1.636	-6.715	-5.285	-1.612	-6.897
Pt_3Ru_1	-4.741	-1.133	-5.874	-5.581	-1.952	-7.533
Ir_3Ag_1	-5.595	-1.913	-7.508	-6.264	-2.433	-8.697
Ir_3Au_1	-4.783	-1.340	-6.123	-6.025	-2.286	-8.311
Ir_3Cu_1	-5.843	-2.107	-7.950	-6.272	-2.453	-8.725
Ir_3Pd_1	-5.435	-1.799	-7.234	-6.086	-2.351	-8.437
Ir_3Pt_1	-5.086	-1.635	-6.721	-5.737	-2.176	-7.913
Ir_3Rh_1	-5.736	-2.089	-7.825	-5.648	-1.955	-7.603
Ir_3Ru_1	-5.555	-2.050	-7.605	-5.802	-2.148	-7.950
Rh_3Ag_1	-5.538	-1.906	-7.444	-6.308	-2.567	-8.875
Rh_3Au_1	-4.947	-1.198	-6.145	-5.995	-2.479	-8.474
Rh_3Cu_1	-5.807	-2.118	-7.925	-6.294	-2.601	-8.895
Rh_3Pd_1	-5.515	-1.833	-7.348	-6.049	-2.499	-8.548
Rh_3Pt_1	-6.015	-2.208	-8.223	-5.710	-2.290	-8.000
Rh_3Ir_1	-5.845	-2.206	-8.051	-5.655	-2.085	-7.740
Rh_3Ru_1	-5.623	-2.164	-7.787	-5.942	-2.376	-8.318

Table S8. The site types and binding atoms of N and O binding configurations on the alloy (100) facets.

	N binding		**O binding**	
	Site type	**Binding atoms**	**Site type**	**Binding atoms**
Ag_3Au_1	4-fold	['Au','Au', 'Ag', 'Ag']	4-fold	['Au','Au', 'Ag', 'Ag']
Ag_3Cu_1	4-fold	['Ag', 'Ag','Cu', 'Cu']	4-fold	['Ag', 'Ag','Cu', 'Cu']
Ag_3Pd_1	4-fold	['Ag', 'Ag','Pd','Pd']	4-fold	['Ag', 'Ag','Pd','Pd']
Ag_3Pt_1	4-fold	['Ag', 'Ag', 'Pt','Pt']	4-fold	['Pt', 'Pt', 'Ag', 'Ag']
Ag_3Ir_1	4-fold	['Ag', 'Ag', 'Ir','Ir']	4-fold	['Ag', 'Ag', 'Ir','Ir']
Ag_3Rh_1	4-fold	['Ag', 'Ag', 'Rh','Rh']	4-fold	['Ag', 'Ag', 'Rh','Rh']
Ag_3Ru_1	4-fold	['Ag', 'Ag', 'Ru','Ru']	4-fold	['Ag', 'Ag', 'Ru','Ru']
Au_3Ag_1	4-fold	['Ag', 'Ag', 'Au', 'Au']	4-fold	['Ag', 'Ag', 'Au', 'Au']
Au_3Cu_1	4-fold	['Au', 'Au', 'Cu', 'Cu']	4-fold	['Au', 'Au', 'Cu', 'Cu']
Au_3Pd_1	4-fold	['Pd', 'Pd', 'Au', 'Au']	4-fold	['Pd', 'Pd', 'Au', 'Au']
Au_3Pt_1	4-fold	['Pt', 'Pt', 'Au', 'Au']	bridge	['Pt', 'Au']
Au_3Ir_1	4-fold	['Au', 'Au', 'Ir', 'Ir']	4-fold	['Ir', 'Ir']
Au_3Rh_1	4-fold	['Rh','Rh', 'Au', 'Au']	4-fold	['Rh', 'Rh']
Au_3Ru_1	4-fold	['Au', 'Au', 'Ru','Ru']	4-fold	['Ru', 'Ru']
Cu_3Ag_1	4-fold	['Ag', 'Ag', 'Cu', 'Cu']	4-fold	['Ag', 'Ag', 'Cu', 'Cu']
Cu_3Au_1	4-fold	['Au', 'Au', 'Cu', 'Cu']	4-fold	['Au', 'Au', 'Cu', 'Cu']
Cu_3Pd_1	4-fold	['Pd', 'Pd', 'Cu', 'Cu']	4-fold	['Pd', 'Pd', 'Cu', 'Cu']
Cu_3Pt_1	4-fold	['Pt', 'Pt', 'Cu', 'Cu']	4-fold	['Pt', 'Pt', 'Cu', 'Cu']
Cu_3Ir_1	4-fold	['Cu', 'Cu', 'Ir', 'Ir']	bridge	['Cu', 'Ir']
Cu_3Rh_1	4-fold	['Cu', 'Cu', 'Rh', 'Rh']	4-fold	['Rh', 'Rh', 'Cu', 'Cu']
Cu_3Ru_1	4-fold	['Ru', 'Ru', 'Cu', 'Cu']	bridge	['Ru', 'Cu']
Pd_3Ag_1	4-fold	['Pd', 'Pd', 'Ag','Ag',]	4-fold	['Pd', 'Pd', 'Ag', 'Ag']
Pd_3Au_1	4-fold	['Pd', 'Pd', 'Au', 'Au']	4-fold	['Pd', 'Pd', 'Au', 'Au']

Pd_3Cu_1	4-fold	['Pd', 'Pd', 'Cu', 'Cu']	4-fold	['Pd', 'Pd', 'Cu', 'Cu']
Pd_3Pt_1	4-fold	['Pd', 'Pd', 'Pt','Pt']	bridge	['Pt', 'Pd']
Pd_3Ir_1	4-fold	['Pd', 'Pd', 'Ir', 'Ir']	4-fold	['Pd', 'Pd', 'Ir', 'Ir']
Pd_3Rh_1	4-fold	['Rh', 'Rh', 'Pd', 'Pd']	4-fold	['Rh', 'Rh', 'Pd', 'Pd']
Pd_3Ru_1	4-fold	['Ru', 'Ru', 'Pd', 'Pd']	4-fold	['Ru', 'Ru', 'Pd', 'Pd']
Pt_3Ag_1	4-fold	['Pt', 'Pt', 'Ag', 'Ag']	4-fold	['Pt', 'Pt', 'Ag', 'Ag']
Pt_3Au_1	4-fold	['Pt', 'Pt', 'Au', 'Au']	bridge	['Pt', 'Au']
Pt_3Cu_1	4-fold	['Pt', 'Pt', 'Pt', 'Pt']	bridge	['Pt', 'Pt']
Pt_3Pd_1	4-fold	['Pt', 'Pt', 'Pd', 'Pd']	bridge	['Pt', 'Pd']
Pt_3Ir_1	bridge	['Pt', 'Ir']	bridge	['Pt', 'Ir']
Pt_3Rh_1	4-fold	['Pt', 'Pt', 'Rh', 'Rh']	bridge	['Pt', 'Rh']
Pt_3Ru_1	4-fold	['Pt', 'Pt', 'Pt', 'Pt']	bridge	['Pt', 'Pt']
Ir_3Ag_1	4-fold	['Ag', 'Ag', 'Ir', 'Ir']	top	['Ir']
Ir_3Au_1	4-fold	['Au', 'Au', 'Ir', 'Ir']	top	['Ir']
Ir_3Cu_1	4-fold	['Cu', 'Cu', 'Ir', 'Ir']	4-fold	['Cu', 'Cu', 'Ir', 'Ir']
Ir_3Pd_1	4-fold	['Pd', 'Pd', 'Ir', 'Ir']	top	['Ir']
Ir_3Pt_1	4-fold	['Pt', 'Pt', 'Ir', 'Ir']	bridge	['Pt', 'Ir']
Ir_3Rh_1	4-fold	['Rh', 'Rh', 'Ir', 'Ir']	bridge	['Rh', 'Ir']
Ir_3Ru_1	4-fold	['Ir', 'Ir', 'Ir', 'Ir']	bridge	['Ir', 'Ir']
Rh_3Ag_1	4-fold	['Rh', 'Rh', 'Ag', 'Ag']	4-fold	['Rh', 'Rh', 'Ag', 'Ag']
Rh_3Au_1	4-fold	['Rh', 'Rh', 'Au', 'Au']	4-fold	['Rh', 'Rh', 'Au', 'Au']
Rh_3Cu_1	4-fold	['Rh', 'Rh', 'Cu', 'Cu']	4-fold	['Rh', 'Rh', 'Cu', 'Cu']
Rh_3Pd_1	4-fold	['Rh', 'Rh', 'Pd', 'Pd']	4-fold	['Rh', 'Rh', 'Pd', 'Pd']
Rh_3Pt_1	4-fold	['Rh', 'Rh', 'Rh', 'Rh']	4-fold	['Rh', 'Rh', 'Rh', 'Rh']
Rh_3Ir_1	4-fold	['Rh', 'Rh', 'Rh', 'Rh']	4-fold	['Rh', 'Rh', 'Rh', 'Rh']
Rh_3Ru_1	4-fold	['Rh', 'Rh', 'Rh', 'Rh']	4-fold	['Rh', 'Rh', 'Rh', 'Rh']

Note: The inconsistence between site types and the numbers of binding atoms for the O binding on (100) of Au_3Ir_1, Au_3Rh_1 and Au_3Ru_1 is because the surface reconstruction makes the adsorbed oxygen only bind with diagonal two atoms of 4-fold sites.

Table S9. The site types and binding atoms of N and O binding configurations on the alloy (111) facets.

	N binding		O binding	
	Site type	Binding atoms	Site type	Binding atoms
Ag_3Au_1	3-fold	['Au', 'Ag', 'Ag']	3-fold	['Au', 'Ag', 'Ag']
Ag_3Cu_1	3-fold	['Ag', 'Ag', 'Cu']	3-fold	['Ag', 'Ag', 'Cu']
Ag_3Pd_1	3-fold	['Ag', 'Ag', 'Pd']	3-fold	['Ag', 'Ag', 'Pd']
Ag_3Pt_1	3-fold	['Ag', 'Ag', 'Pt']	3-fold	['Ag', 'Ag', 'Pt']
Ag_3Ir_1	top	['Ir']	top	['Ir']
Ag_3Rh_1	3-fold	['Ag', 'Ag', 'Rh']	3-fold	['Ag', 'Ag', 'Rh']
Ag_3Ru_1	3-fold	['Ag', 'Ag', 'Ru']	3-fold	['Ag', 'Ag', 'Ru']
Au_3Ag_1	3-fold	['Au', 'Au', 'Au']	3-fold	['Au', 'Au', 'Au']
Au_3Cu_1	3-fold	['Au', 'Au', 'Cu']	3-fold	['Au', 'Au', 'Cu']

Au_3Pd_1	3-fold	['Pd', 'Au', 'Au']	3-fold	['Pd', 'Au', 'Au']
Au_3Pt_1	3-fold	['Au', 'Au', 'Pt']	3-fold	['Au', 'Au', 'Pt']
Au_3Ir_1	3-fold	['Au', 'Au', 'Ir']	top	['Ir']
Au_3Rh_1	3-fold	['Rh', 'Au', 'Au']	3-fold	['Rh', 'Au', 'Au']
Au_3Ru_1	3-fold	['Au', 'Au', 'Ru']	top	['Ru']
Cu_3Ag_1	3-fold	['Cu', 'Cu', 'Cu']	3-fold	['Cu', 'Cu', 'Cu']
Cu_3Au_1	3-fold	['Cu', 'Cu', 'Cu']	3-fold	['Cu', 'Cu', 'Cu']
Cu_3Pd_1	3-fold	['Cu', 'Cu', 'Cu']	3-fold	['Cu', 'Cu', 'Cu']
Cu_3Pt_1	3-fold	['Cu', 'Cu', 'Pt']	3-fold	['Cu', 'Cu', 'Pt']
Cu_3Ir_1	3-fold	['Cu', 'Cu', 'Ir']	3-fold	['Cu', 'Cu', 'Ir']
Cu_3Rh_1	3-fold	['Cu', 'Cu', 'Rh']	3-fold	['Cu', 'Cu', 'Rh']
Cu_3Ru_1	3-fold	['Cu', 'Cu', 'Ru']	3-fold	['Cu', 'Cu', 'Ru']
Pd_3Ag_1	3-fold	['Pd', 'Pd', 'Pd']	3-fold	['Pd', 'Pd', 'Pd']
Pd_3Au_1	3-fold	['Pd', 'Pd', 'Pd']	3-fold	['Pd', 'Pd', 'Pd']
Pd_3Cu_1	3-fold	['Pd', 'Pd', 'Pd']	3-fold	['Pd', 'Pd', 'Pd']
Pd_3Pt_1	3-fold	['Pd', 'Pt', 'Pd']	3-fold	['Pd', 'Pt', 'Pd']
Pd_3Ir_1	3-fold	['Ir', 'Pd', 'Pd']	3-fold	['Ir', 'Pd', 'Pd']
Pd_3Rh_1	3-fold	['Pd', 'Pd', 'Rh']	3-fold	['Pd', 'Pd', 'Rh']
Pd_3Ru_1	3-fold	['Pd', 'Pd', 'Ru']	3-fold	['Pd', 'Pd', 'Ru']
Pt_3Ag_1	3-fold	['Pt', 'Pt', 'Pt']	3-fold	['Pt', 'Pt', 'Pt']
Pt_3Au_1	3-fold	['Pt', 'Pt', 'Pt']	3-fold	['Pt', 'Pt', 'Pt']
Pt_3Cu_1	3-fold	['Pt', 'Pt', 'Pt']	3-fold	['Pt', 'Pt', 'Pt']
Pt_3Pd_1	3-fold	['Pt', 'Pt', 'Pt']	3-fold	['Pt', 'Pt', 'Pt']
Pt_3Ir_1	3-fold	['Pt', 'Pt', 'Ir']	3-fold	['Pt', 'Pt', 'Ir']
Pt_3Rh_1	3-fold	['Pt', 'Rh', 'Pt']	3-fold	['Pt', 'Rh', 'Pt']
Pt_3Ru_1	3-fold	['Pt', 'Ru', 'Pt']	3-fold	['Pt', 'Ru', 'Pt']
Ir_3Ag_1	3-fold	['Ir', 'Ir', 'Ir']	3-fold	['Ir', 'Ir', 'Ir']
Ir_3Au_1	3-fold	['Ir', 'Ir', 'Ir']	3-fold	['Ir', 'Ir', 'Ir']
Ir_3Cu_1	3-fold	['Ir', 'Ir', 'Ir']	3-fold	['Ir', 'Ir', 'Ir']
Ir_3Pd_1	3-fold	['Ir', 'Ir', 'Ir']	3-fold	['Ir', 'Ir', 'Ir']
Ir_3Pt_1	3-fold	['Ir', 'Ir', 'Ir']	3-fold	['Ir', 'Ir', 'Ir']
Ir_3Rh_1	3-fold	['Ir', 'Ir', 'Ir']	3-fold	['Ir', 'Ir', 'Ir']
Ir_3Ru_1	3-fold	['Ir', 'Ir', 'Ru']	3-fold	['Ir', 'Ir', 'Ru']
Rh_3Ag_1	3-fold	['Rh', 'Rh', 'Rh']	3-fold	['Rh', 'Rh', 'Rh']
Rh_3Au_1	3-fold	['Rh', 'Rh', 'Rh']	3-fold	['Rh', 'Rh', 'Rh']
Rh_3Cu_1	3-fold	['Rh', 'Rh', 'Rh']	3-fold	['Rh', 'Rh', 'Rh']
Rh_3Pd_1	3-fold	['Rh', 'Rh', 'Rh']	3-fold	['Rh', 'Rh', 'Rh']
Rh_3Pt_1	3-fold	['Rh', 'Rh', 'Rh']	3-fold	['Rh', 'Rh', 'Rh']
Rh_3Ir_1	3-fold	['Ir', 'Rh', 'Rh']	3-fold	['Ir', 'Rh', 'Rh']
Rh_3Ru_1	3-fold	['Rh', 'Rh', 'Ru']	3-fold	['Rh', 'Rh', 'Ru']

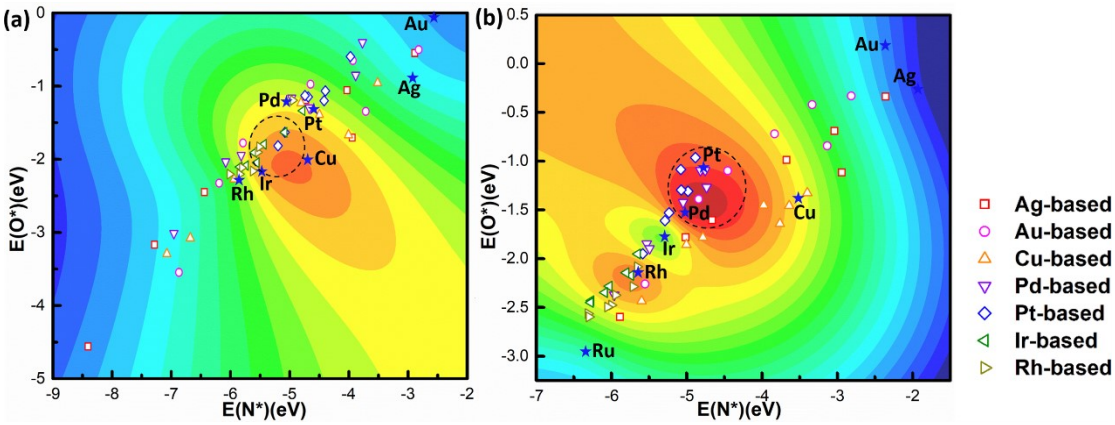

Fig. S8. The distribution of the alloyed catalysts on the contours of N_2 reactivity.

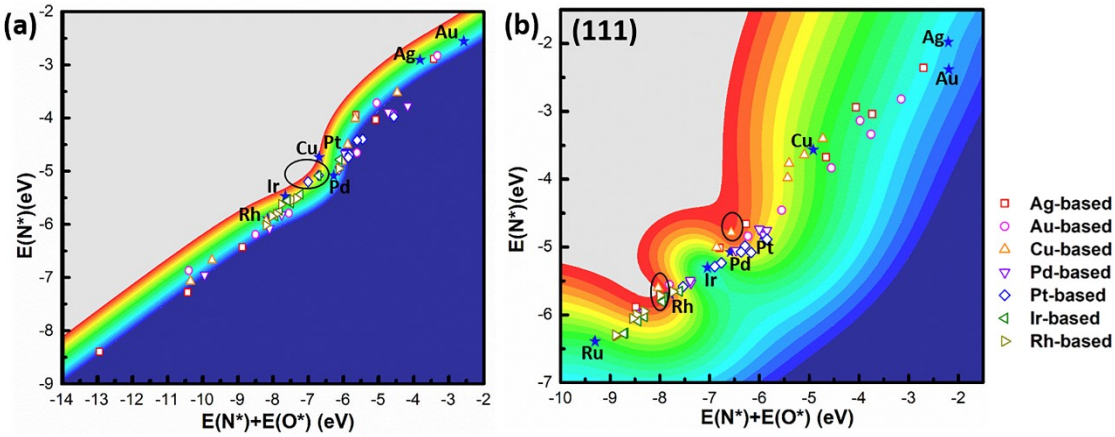

Fig. S9. The distribution of the alloyed catalysts on the contours of N_2 selectivity.

Table S10. The obtained alloyed catalysts with (100) facets.

NH_3 oxidation		N_2 generation			N_2 selectivity		
	E(N*)		E(N*)	E(O*)		E(N*)+E(O*)	E(N*)
Au_3Pd_1	-3.934	Pt_3Ir_1	-5.198	-1.819	Pt_3Ir_1	-7.017	-5.198
Au_3Pt_1	-4.650	Ir_3Pt_1	-5.086	-1.635	Ir_3Pt_1	-6.721	-5.086
Cu_3Ag_1	-4.009	Pt_3Rh_1	-5.079	-1.636	Pt_3Rh_1	-6.715	-5.079
Cu_3Pd_1	-4.499	Ir_3Pd_1	-5.435	-1.799			
Cu_3Pt_1	-4.811	Rh_3Pd_1	-5.515	-1.833			
Pd_3Cu_1	-4.673	Rh_3Ag_1	-5.538	-1.906			
Pd_3Pt_1	-4.968	Ir_3Ag_1	5.595	-1.913			
Pt_3Ag_1	-4.397	Ir_3Au_1	-4.783	-1.340			
Pt_3Au_1	-3.975						
Pt_3Cu_1	-4.420						
Pt_3Pd_1	-4.689						
Pt_3Rh_1	-5.079						
Pt_3Ru_1	-4.741						
Ir_3Au_1	-4.783						
Ir_3Pt_1	-5.086						

Rh_3Au_1	-4.947					

Table S11. The obtained alloyed catalysts with (111) facets.

NH_3 oxidation		N_2 generation			N_2 selectivity		
	$E(N^*)$		$E(N^*)$	$E(O^*)$		$E(N^*)+E(O^*)$	$E(N^*)$
Ag_3Ir_1	-5.010	Au_3Ir_1	-4.838	-1.390	Cu_3Rh_1	-6.569	-4.782
Ag_3Rh_1	-4.658	Au_3Rh_1	-4.453	-1.099	Cu_3Ru_1	-8.035	-5.596
Au_3Ir_1	-4.838	Pd_3Ag_1	-4.817	-1.096	Ir_3Pt_1	-7.913	-5.737
Au_3Rh_1	-4.453	Pd_3Au_1	-4.752	-1.095	Ir_3Ru_1	-7.950	-5.802
Cu_3Pt_1	-3.976	Pd_3Cu_1	-4.733	-1.269	Rh_3Pt_1	-8.000	-5.710
Cu_3Ir_1	-5.001	Pd_3Pt_1	-5.046	-1.424			
Cu_3Rh_1	-4.782	Pt_3Ag_1	-5.076	-1.086			
Pd_3Ag_1	-4.817	Pt_3Au_1	-4.882	-0.964			
Pd_3Au_1	-4.752	Pt_3Cu_1	-4.980	-1.309			
Pd_3Cu_1	-4.733	Pt_3Pd_1	-5.069	-1.297			
Pd_3Pt_1	-5.046	Ag_3Rh_1	-4.658	-1.608			
Pt_3Ag_1	-5.076						
Pt_3Au_1	-4.882						
Pt_3Cu_1	-4.980						
Pt_3Pd_1	-5.069						

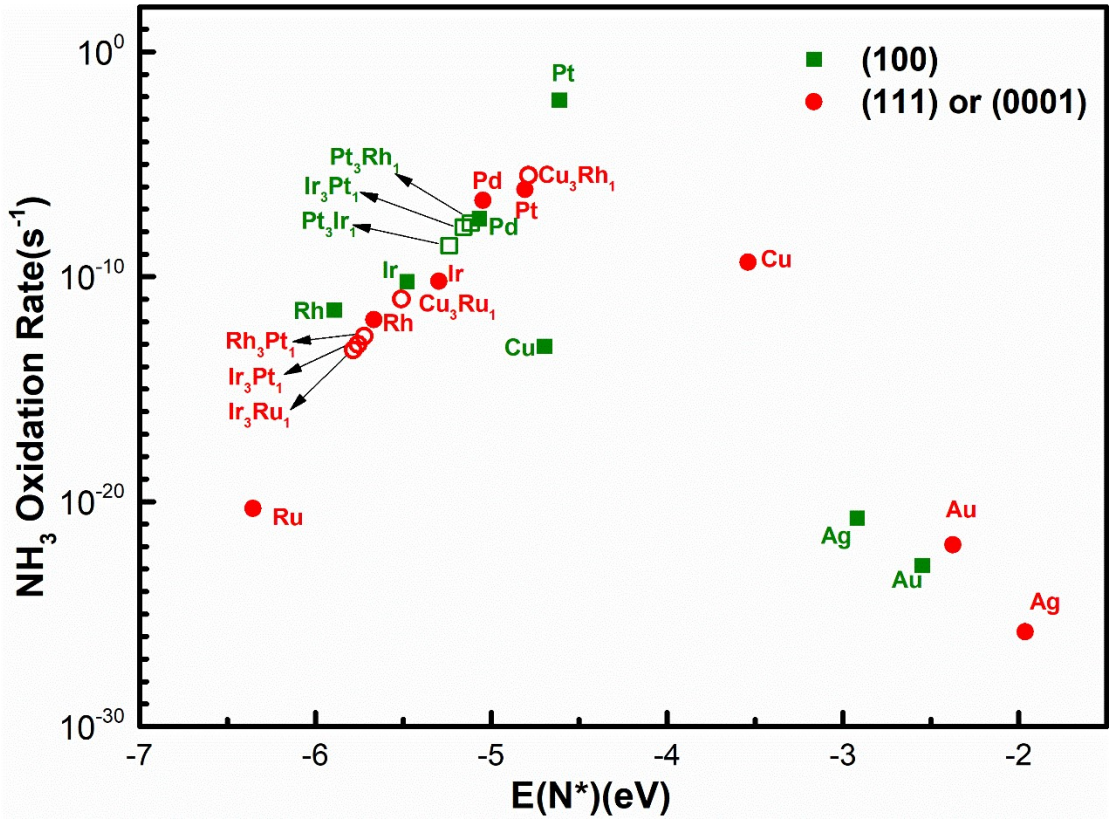

Fig. S10. The distribution of the obtained alloyed catalysts with high selectivity on the volcano relation of NH_3 oxidation activity.

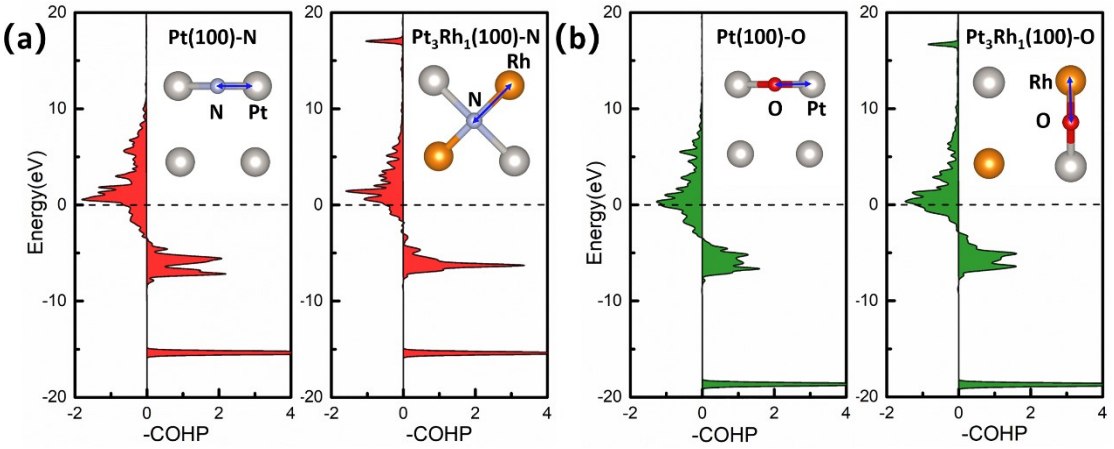

Fig. S11.The COHP bonding analysis on Pt-N, Rh-N, Pt-O and Rh-O for N and O binding on Pt(100) and $Pt_3Rh_1(100)$.

The stability analysis of alloy catalysts.

The formation energy (E_f) of bulk alloy systems is calculated as:

$$E_f = E_{alloy} - N_A E_{A(bulk)} - N_B E_{B(bulk)}$$

Where, E_{alloy}, $E_{A(bulk)}$ and $E_{B(bulk)}$ are bulk energy of alloy, metal A and metal B, respectively and N_A and N_B are the numbers of metallic atoms A and B in alloy systems, respectively.

Table S12. The bulk energy of alloy systems from DFT calculation and corresponding formation energy (E_f) of alloy systems and green items are potential alloy catalysts through high throughput screening based on the catalytic descriptors.

Systems	Energy(eV)	E_f(eV)	Systems	Energy(eV)	E_f (eV)
Ag_3Au_1	-11.469	-0.182	Pd_3Ag_1	-18.399	-0.032
Ag_3Cu_1	-11.411	0.381	Pd_3Au_1	-19.025	-0.167
Ag_3Ir_1	-15.316	1.637	Pd_3Cu_1	-19.566	-0.203
Ag_3Pd_1	-13.587	-0.267	Pd_3Ir_1	-23.960	0.565
Ag_3Pt_1	-14.197	-0.022	Pd_3Pt_1	-21.852	-0.106
Ag_3Rh_1	-14.486	0.898	Pd_3Rh_1	-22.622	0.333
Ag_3Ru_1	-15.059	2.338	Pd_3Ru_1	-24.084	0.884
Au_3Ag_1	-12.463	-0.195	Pt_3Ag_1	-20.776	0.158
Au_3Cu_1	-13.231	0.032	Pt_3Au_1	-21.121	0.304
Au_3Ir_1	-16.995	1.430	Pt_3Cu_1	-22.266	-0.336
Au_3Pd_1	-15.180	-0.388	**Pt_3Ir_1**	**-26.764**	**0.328**
Au_3Pt_1	-15.615	0.033	Pt_3Pd_1	-23.563	-0.105
Au_3Rh_1	-16.231	0.625	**Pt_3Rh_1**	**-25.526**	**-0.004**
Au_3Ru_1	-17.056	1.813	Pt_3Ru_1	-27.255	0.280
Cu_3Ag_1	-13.094	0.690	Rh_3Ag_1	-23.349	1.211
Cu_3Au_1	-14.061	0.213	Rh_3Au_1	-24.190	0.860
Cu_3Ir_1	-19.491	0.450	Rh_3Cu_1	-25.196	0.359

Cu_3Pd_1	-16.681	-0.374	Rh_3Ir_1	-30.794	-0.077
Cu_3Pt_1	-17.640	-0.477	Rh_3Pd_1	-26.704	0.379
Cu_3Rh_1	**-18.252**	**3.608**	**Rh_3Pt_1**	**-27.986**	**-0.047**
Cu_3Ru_1	**-19.236**	**1.148**	Rh_3Ru_1	-31.033	0.127
Ir_3Ag_1	-27.344	1.925			
Ir_3Au_1	-27.996	1.764			
Ir_3Cu_1	-29.441	0.824			
Ir_3Pd_1	-31.114	0.679			
Ir_3Pt_1	**-32.257**	**0.392**			
Ir_3Rh_1	-33.902	-0.045			
Ir_3Ru_1	-36.040	-0.170			

Reference:

1 H. Ma, W. F. Schneider, ACS Catal., 2019, 9, 2407−2414.

2 H. Ma, W. Schneider, J. Catal., 2020, 383, 322-330.